Influence of Morphometric Factors on Quantitation of Paracellular Permeability of Intestinal Epithelia *In Vitro*

Andrew Collett,[1] David Walker,[1] Erika Sims,[1] Yan-Ling He,[2] Peter Speers,[1] John Ayrton,[3] Malcolm Rowland,[2] and Geoffrey Warhurst[1,4]

Received November 12, 1996; accepted March 1997

Purpose. The relative contribution of the small and large intestine to paracellular absorption is a subject of some controversy. Direct comparison of paracellular permeability in different epithelia is complicated by variations in junctional density and/or the absorptive surface area.

Methods. This study used a combination of morphometric analyses and *in vitro* absorption studies to define permeability characteristics in relation to the amount of paracellular pathway present in rat ileum, colon and the model epithelium, Caco-2.

Results. Mucosal to serosal amplification was higher in ileum (3.9) than colon (1.9) or Caco-2 (1). Tight junctional density (lp) of ileal crypts was ≈3 fold greater (91 m/cm^2) than that measured in ileal villi, colonic surface and crypt cells or Caco-2 monolayers (34–37 m/cm^2). However, when the relative contributions of the crypts and villi was taken into account there was no significant difference in the mean lp per mucosal area for the three epithelia studied. Using these data to correct for morphometric differences the permeabilities of a range of small hydrophilic molecules (atenolol, D-PheAsp and PEG oligomers MW 282-634) was measured. Permeability of rat ileum and colon were virtually identical for all compounds studied. In contrast, Caco-2 monolayers showed a significantly lower permeability than intestinal tissues with the difference increasing markedly with molecular size.

Conclusions. These studies suggest the importance of accounting for morphological variation when comparing the permeability characteristics of different epithelial systems.

KEY WORDS: intestinal permeability; morphometric analysis; paracellular permeability; drug absorption; Caco-2 cells.

INTRODUCTION

Passive transport though intercellular tight junctions in the intestinal epithelium, known as the paracellular route, is considered to be the major pathway for absorption of small hydrophilic molecules, including some drugs (1,2). Comparison of the paracellular permeability characteristics of different intestinal regions both within and between species is crucial to our mechanistic understanding of paracellular transport and for the development of model systems which can more accurately predict intestinal drug absorption (3). Such comparisons are complicated by morphological variation resulting in marked differences in the total surface area available for absorption and/or the density of tight junctions (4,5). Partly as a result of this, there is considerable variance in the literature on the permeability characteristics of different intestinal regions (6,7,8). In the absence of morphometric data only relative comparisons of permeability between epithelial systems can be made. In addition, subtle differences in the permeability characteristics of tight junctions in different epithelia may be masked by these factors. Previous studies have identified the morphometric parameters which can be used to define the paracellular pathway (4,9,10). However, there have been few attempts to correlate morphometric parameters and permeability as a means of comparing the absorptive properties of different epithelia.

In the present study, morphometric analyses of mucosal surface amplification and tight junctional density have been used in conjunction with *in vitro* permeability studies of several hydrophilic compounds to compare the permeability characteristics of rat ileum and colon. In addition, using similar techniques we have examined the permeability of Caco-2 epithelial monolayers which have been widely proposed as a model of intestinal paracellular drug absorption (11,12).

MATERIALS AND METHODS

Compounds

[^{3}H]-D-Phenylalanine-Aspartic acid (D-PheAsp) was custom synthesized by Zeneca, UK. [^{3}H]-atenolol and [^{14}C]-polyethylene glycol 400 (PEG400) was supplied by Amersham, UK. D-PheAsp was synthesized in house. All other compounds were analytical grade. The basic physical characteristics of the compounds used in the permeability experiments are shown in Table I.

Tissue Culture

Caco-2 cells (passage 90–110) were cultured as described previously (13). For drug transport studies, cells were seeded on 12mm polycarbonate filter cell culture inserts (Transwell, Costar, High Wycombe, UK) at a density of 1×10^5 cells/cm^2. Culture media was changed every 2 days and the cultures were

Table I. The Molecular Weight, Size and Log Octanol/Water Partition Coefficient (log Kp) of the Paracellular Probes Used in This Study

Drug	Molecular wt	Size (Å)	log Kp
Atenolol	266	4.80	−2.14
D-PheAsp	280	4.88	N/A
PEG282	282	3.81	−2.21
PEG376	376	4.30	−3.08
PEG502	502	4.94	−3.40
PEG634	634	5.51	−3.70

Note: The PEG molecular size is based on experimentally determined data from Ruddy and Hadzija (1992) (14). The size of atenolol and PheAsp was calculated from their molecular weight. The log Kp for atenolol is taken from LogKOW Technical Database Services Inc. New York and for the PEG oligomers from Ma *et al.* Gastroenterology **98:** 38–46 (1990).

[1] Department of Medicine (University of Manchester School of Medicine), Hope Hospital, Salford M6 8HD, UK.
[2] Department of Pharmacy, University of Manchester, Manchester M13 9PL, UK.
[3] GlaxoWellcome, Greenford, Middlesex, UK.
[4] To whom correspondence should be addressed. (e-mail: gwarhurst@fs1.ho.man.uk.ac)

used for permeability studies 22–27 days after seeding. Development of transepithelial electrical resistance (R_t) was monitored at 37°C using an Evometer (World Precision Instruments, Sarasota, USA.) fitted with 'chop stick' electrodes.

HPLC Analysis of Test Compounds

D-PheAsp, atenolol and PEG400 were analyzed using a high performance liquid chromatography system (Spectra Series AS300, USA) equipped with a radiomatic detector (Flo-One\Beta, Canberra Packard, USA) to ascertain that all the radio-label was associated with the parent compound. The stationary phase was Partisil ODS1 with 10mm particle size (250mm × 4.6mm i.d., Thames Chromatography, UK) and a mobile phase of 90% 50mM phosphoric acid (pH 3.0) and 10% methanol. The flow rate was 1.5ml/min and column temperature was maintained at 30°C. This technique resolved a total of 13 oligomers from PEG400 with molecular weights ranging from 194 to 723 Daltons. Characterization of the molecular weight of each oligomer was accomplished by reference to the retention times of two standard oligomers of molecular weight 282 and 414 detected by refractometry. In this study four oligomers of molecular weight 282, 376, 502 and 634 were quantified by measurement of peak area.

Transport Studies

Rat Intestine

All procedures involving animals conformed to current UK Home Office legislation and adhered to the Principles of Laboratory Care (NIH publication #85-23, 1985). Non-fasting male Sprague-Dawley rats were stunned and killed by cervical dislocation. The ileum and colon were immediately removed, washed and stripped of muscle layers by blunt dissection. Segments of the mucosa were mounted in Ussing chambers (0.64cm^2 surface area) and bathed on the mucosal and serosal aspects with 4 mls serum-free Dulbecco's modified Eagles medium (SFDM) (GibcoBRL, Life Technologies, Paisley, UK) pH 7.4 at 37°C under continuous oxygenation. This procedure was completed within 20 mins of removal of tissue from the animal. Spontaneous tissue potential difference (PD) and transepithelial electrical resistance (R_t), measured as the deflection in PD caused by a 100μA current pulse, were monitored periodically throughout the experiment. At all other times the tissue was maintained under short circuit conditions. Only data from tissues in which electrical parameters remained within 15% of the initial stabilized values throughout the period of the experiment were included.

After a 45 min equilibration period, labelled and unlabelled compound were added to the mucosal (apical) chamber to give a final concentration of 0.1mM. A 100 μl sample was removed from the mucosal side to determine the initial isotopic concentration. For studies using D-PheAsp and atenolol, serosal samples (1ml) were removed for each of 3 successive time periods of 30–60 min and replaced with fresh SFDM. In the case of PEG400 a single time period of 3 hr was used to achieve the sensitivity necessary to detect the individual PEG oligomers by HPLC. Initial experiments using shorter time intervals and quantitating total radioactivity were performed to ensure that PEG400 permeability was linear with time during this period. All ^{3}H or ^{14}C activities were determined by HPLC analysis as outlined above.

Caco-2 Monolayers

Drug transport across Caco-2 was measured by a method similar to that described previously (13). Briefly, epithelial cell layers were removed from the growth medium, washed twice in SFDM and placed in a 12 well plate. Aliquots of SFDM were added to the apical (0.5 ml) and basolateral (1.5 ml) compartments and cell layers were left for 60 min to equilibrate. Aliquots (100 μl) were removed from the apical reservoir and replaced with an equal volume of a solution of ^{3}H- or ^{14}C-labelled and unlabelled compound to give a final concentration of 0.1 mM. After each incubation period (30–45 min) the cell culture insert was moved to the next well containing a fresh 1.5 ml aliquot of SFDM. The basolateral solution from each flux period and 20 μl apical samples taken at the beginning and end of each experiment were analyzed by HPLC analysis as outlined above.

For studies involving a Ca^{2+} removal step, culture inserts were washed three times with a SFDM solution containing 2.5mM ethylene glycol-bis-(β-aminoethyl ether)-N,N,N′N′-tetraacetic acid (EGTA) and incubated in this medium on both apical and basolateral sides for 20 min after which time extracellular Ca^{2+} was replaced. This procedure has previously been shown to cause a transient and fully reversible decrease in monolayer resistance and a reversible increase in paracellular permeability (13).

Permeability (Papp) values expressed as cm/sec were obtained according to the equation:

$$\text{Papp} = \frac{dQ/dt}{A \cdot C} \quad (1)$$

where: dQ/dt = rate at which the compound appears in the basolateral compartment; A = surface area of the tissue/monolayer; C = initial concentration of compound in apical compartment.

Morphometric Analysis

Samples of rat ileum and colon, stripped and mounted for Ussing chamber studies, and Caco-2 monolayers were prepared for electron microscopic analysis using standard techniques as described by Marcial *et al.* (9).

Amplification Ratio

Transversely and longitudinally oriented sections of mounted ileum and colon were used to determine the mucosal to serosal amplification ratio. Morphometric analysis was performed using a Videoplan Morphometry Unit (Kontron, Watford, UK.) interfaced to an Olympus BH-2 light microscope (Olympus, London, UK.) with a video camera attachment. The on-screen images of the sections were measured in real-time using a morphometry stylus on a digital tablet calibrated with a stage graticule.

A morphometric technique which accounts for the true 3-dimensional geometry of the mucosa was devised. This is illustrated for the ileum in Fig. 1. From oriented tissue blocks, sequential transverse sections were taken every 10 μm from

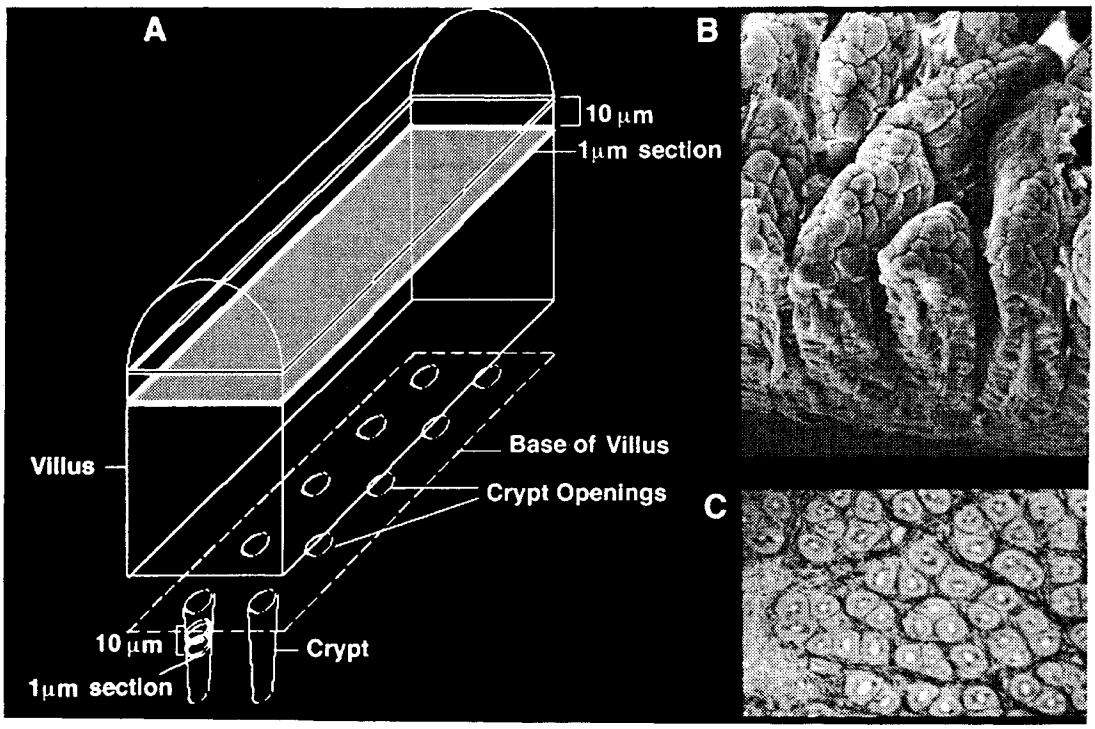

Fig. 1. Measurement of mucosal surface amplification **A** Schematic representation of ileal villus and crypt to illustrate the method of sectioning and quantification of mucosal surface as detailed in Materials and Methods. **B** Scanning electron micrograph (140×) showing shape and orientation of ileal villi. **C** Light micrograph (400×) of longitudinal section illustrating the mouth of the crypts after sequential sectioning to the base of the villi. On average 8–10 crypts were associated with each villus.

the base of the crypts to the tips of the villi so that both crypts and villi appear in cross-section (Fig. 1A). The crypt luminal surface length was measured in each successive section until the mouth opened at the surface (Fig. 1C). Similarly, the periphery of the transversely sectioned villi was measured in successive sections until the tip of the villus was reached. To calculate surface area, each luminal surface length value was multiplied by 10 and the sum of these values taken. Measurements were repeated for all the crypts and villi within each section and the mean crypt and villus surface area calculated (as shown in equation 2). The total mucosal area calculated is divided by the flat, underlying serosal area to give a value which represents the fold amplification of mucosal area compared to the serosal area (see equation 2). A similar approach was taken for the colon except that, being devoid of villi, measurements were taken only from the base of the crypt to the crypt opening.

$$\text{Surface amplification} = \frac{D\cdot(l_c\cdot n_c)\cdot y_c + D\cdot(l_v\cdot n_v)\cdot y_v}{\text{serosal area}} \quad (2)$$

l_c = length round the periphery of crypt sections
l_v = length round the periphery of villi sections
n_c = number of sections per crypt
n_v = number of sections per villi
y_c = number of crypts per unit serosal area
y_v = number of villi per unit serosal area
D = distance between sections (10μm)

Measurement of Junctional Density (lp)

Thin (1μm) sections of silver interference color were used to estimate tight junction density (length of tight junction per unit surface area). One section per grid and one grid per intestinal sample was used for quantitative analysis. All visible luminal plasma membrane profiles from each section were photographed at a 6,000× magnification on a Phillips 400 electron microscope and the images photographically enlarged to 15,000× (Fig. 2). Between 25–40 micrographs were obtained from a single section. The surface length at the base of the microvilli was measured and the tight junction profiles counted. The number of tight junctions per unit surface length was then calculated to give the linear surface junctional density.

In order to transform the data to length of tight junction per unit surface area (lp), the relationship between linear surface junctional density and lp must be defined. Previous calculations based both on model systems and *in vivo* analysis show that the ratio of lp values to linear surface junctional density values is approximately 2 (9) and this value is used here.

From thin section measurements, the lp for each micrograph was calculated using the following equation:-

$$lp = sa/d \times tj \times 2 \quad (3)$$

where: sa = unit surface area ($1cm^2$); d = length of luminal plasma membrane (μm); tj = number of tight junctions; 2 = ratio constant.

Statistical Analysis

Data are presented as means ± S.E.M. Comparisons were made by application of the Student's *t*-test for unpaired data or where appropriate the Mann-Whitney *U*-test. Values of $p < 0.05$ were taken as significant.

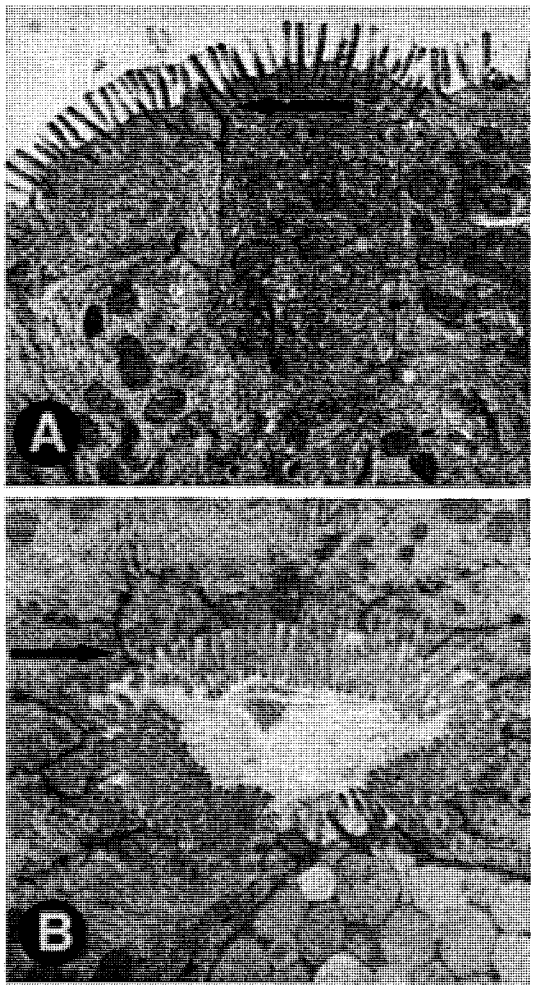

Fig. 2. Measurement of tight junctional density (lp). Transmission electron micrographs of epithelial surface of rat ileal villus (**A**) and crypt (**B**) (original magnification 6000× and photographically enlarged to 15000× in each case) with arrows indicating examples of junctional contacts.

Table II. Morphometric Data

	lp (m/cm^2)		Contribution to total surface area		Mean lp (m/cm^2)
	Villus	Crypt	% Villus	% Crypt	
Ileum	34 ± 3 surface	91 ± 2 crypt	90.5 % surface	9.5 % crypt	39 ± 2
Colon	36 ± 1	37 ± 1	23	77	37 ± 1
Caco-2	—	—	—	—	37 ± 2

Note: Summarizes the length of tight junction (lp) per unit area of epithelium in villi and crypt regions of the ileum and surface cells and crypts in the colon. The mean lp value for ileum, colon and Caco-2 was determined by taking account of the contribution of each region to the overall surface area of the epithelium.

RESULTS

Morphometric Comparison of Rat and Caco-2 Epithelia

Initial studies sought to define rat ileum, colon and Caco-2 monolayers in morphometric terms by measuring relative absorptive area and tight junctional density in each epithelium. Using the approach illustrated in Fig. 1 the three dimensional amplification ratio calculated for ileum (3.9 ± 0.2) was approximately two fold greater than colon (1.9 ± 0.1) for tissues which had been muscle-stripped and mounted in Ussing chambers. Amplification ratios in rat ileum prior to mounting in Ussing chambers was significantly higher (7.2 ± 0.9) than mounted tissues while values for colon were only slightly increased (2.4 ± 0.1). Using the same approach the value for Caco-2 monolayers is by definition 1. The tight junctional density (lp) in ileum and colon was also determined (Table II). Ileal crypts have an approximately 3 fold greater density of tight junctions than the villus region (91 ± 2 m/cm^2 vs 34 ± 3 m/cm^2). However, the contribution of crypts to the total epithelial surface area is relatively small (9.5%) with the result that a mean lp calculated for ileum (39 ± 2 m/cm^2) is similar to the villus value. In the colon, the lp of surface and crypt regions is essentially identical giving a mean lp for colon of 37 ± 1 m/cm^2 (Table II). Mature Caco-2 cell monolayers, considered to be of colonic crypt origin, had an lp value of 37 ± 2 m/cm^2. By combining values for mean lp with the respective amplification ratios for each epithelium, a value corresponding to the total length of tight junction per cm^2 of mounted epithelia was calculated giving 154 m/cm^2 for ileum, 71 m/cm^2 for colon and 37 m/cm^2 for Caco-2 monolayers or a ratio of 4.2 : 1.9 : 1.

Morphometric Correction of Transepithelial Electrical Resistance (Rt)

Measurement of electrical resistance (Rt) is often used as an approximate indicator of the "tightness" of the paracellular pathway and is usually expressed *in vitro* per unit area of mounted tissue (ie. serosal area). This approach shows marked differences between the epithelia with values of 46 ± 2.5 Ω.cm^2 (n = 13) for ileum, 74 ± 4.5 Ω.cm^2 (n = 12) for colon and 310 ± 25 Ω.cm^2 (n = 20) for Caco-2 monolayers. However, Rt values recalculated to take account of surface amplification show much smaller differences between the epithelia (Ileum: 180 Ω.cm^2, Colon: 140 Ω.cm^2, Caco-2: 310 Ω.cm^2.)

Correlation Between Morphometric Parameters and Paracellular Permeability

Further studies investigated whether differences in paracellular permeability between rat and Caco-2 systems could be explained simply in terms of morphometric variation. Fig. 3 shows permeability values for two paracellularly transported compounds, atenolol (AT) and the D-dipeptide D-PheAsp in rat and Caco-2 systems. The measured permeabilities of both compounds across rat ileum were significantly higher than in colon when the values are expressed per cm^2 of serosal area mounted in the flux chamber (Fig. 3). However, when values are adjusted to take account of differences in either mucosal area or the total amount of junctional pathway available in each cm^2 of serosal area, the permeabilities of both regions are similar (Fig. 3 insert). In contrast, the Papp for AT and D-PheAsp across Caco-2 monolayers was significantly lower (by a factor of approximately 8) than rat intestine, even after correction for morphometric differences.

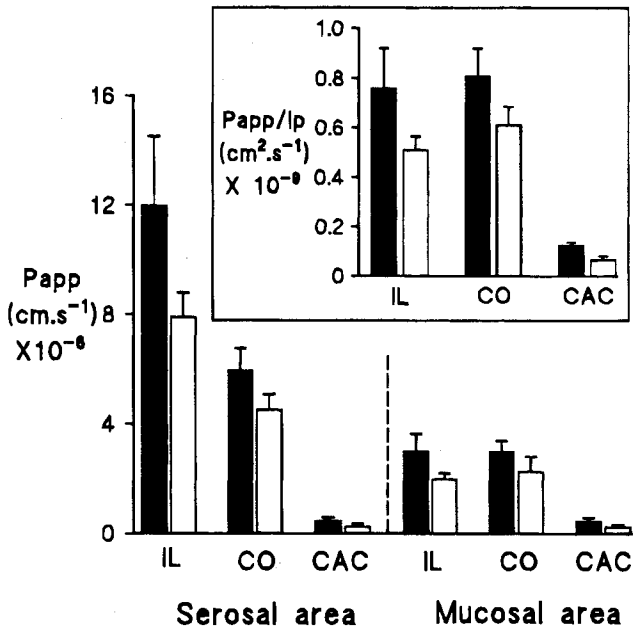

Fig. 3. Permeability of atenolol and PheAsp across rat and Caco-2 epithelia. Data shows mean permeability (Papp) of atenolol (■) and PheAsp (□) across rat ileum (IL), colon (CO) and Caco-2 monolayers (CAC) expressed in terms of serosal or mucosal surface area (calculated as described in Materials and Methods). Insert shows Papp values recalculated to take account of differences in mucosal surface area and mean tight junctional density (lp) and expressed as permeability per unit length of tight junction. Data shown are mean ± SEM for 4–8 experiments in each group.

Defined PEG oligomers were also used to investigate the permeability characteristics of each epithelia in relation to molecular size. Figure 4 shows the permeability of 4 PEG oligomers (of molecular weights 282 to 634) across rat and Caco-2 epithelia. In each case, permeability was corrected for morphometric differences and expressed per unit area of mucosa. For all three epithelia the permeability of PEG oligomers decreased with increasing molecular weight. Rat ileum and colon showed comparable PEG permeabilities for each of the four oligomers suggesting there is no significant difference between the paracellular pathways in these regions. In contrast, while the PEG profile in Caco-2 was qualitatively similar the absolute permeability of PEG oligomers across this epithelium was significantly lower. The difference in permeability between rat and Caco-2 was also much greater as molecular size increased. For PEG282 the intestine was approximately four times more permeable than Caco-2 while for PEG502 rat intestine was about 40-fold more permeable than the cell line.

EGTA treatment is commonly used to increase the permeability of Caco-2 monolayers to compounds transported via the paracellular route (13). Fig. 5 shows the effect of pulse treatment of Caco-2 monolayers with 2.5mM EGTA on the permeability of the various compounds in comparison to rat ileum. Under these conditions, the permeability of Caco-2 monolayers closely mimicked the rat ileum both in terms of absolute permeability and molecular weight dependence.

DISCUSSION

In this study we have directly compared the *in vitro* permeability of different sized paracellular probes across epithelia from the rat ileum and colon and the human colonic cell line Caco-2. Morphometric parameters relating to total absorptive surface area and mean density of tight junctions have been used to "normalize" *in vitro* permeability data and facilitate a direct comparison between these systems.

Using this approach with small hydrophilic molecules (atenolol, D-PheAsp) and a multicomponent preparation of defined PEG oligomers, the "normalized" permeabilities (ie per unit of mucosal area or junctional pathway) of rat ileum and colon were found to be essentially identical. Using the same calculation, the permeability of these compounds across Caco-

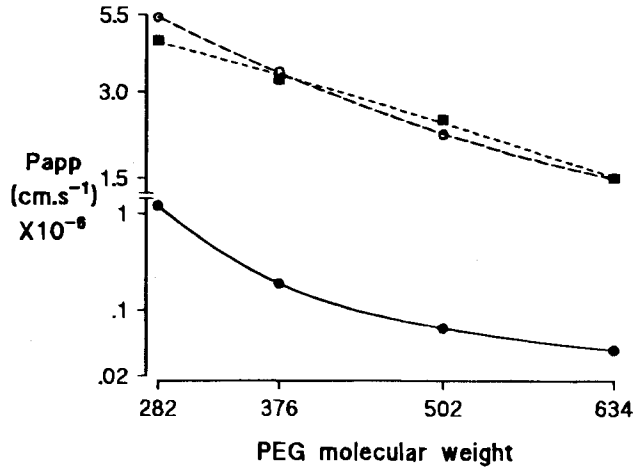

Fig. 4. Permeability of PEG oligomers across rat and Caco-2 epithelia after correction for differences in surface amplification. Figure shows Papp of PEG molecules of defined molecular size across rat ileum (○), rat colon (■) and Caco-2 (●) expressed per unit of mucosal surface area. Data shown are mean of 4–5 experiments in each group.

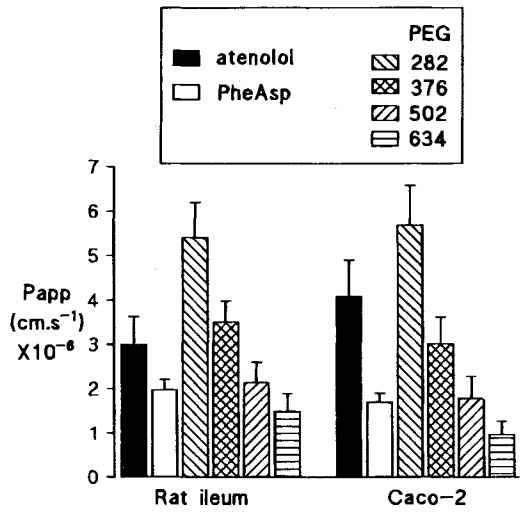

Fig. 5. Comparison of permeability profile of EGTA-treated Caco-2 monolayers with rat ileum. The permeabilities (Papp) for atenolol, D-PheAsp and PEG oligomers are expressed per mucosal surface area in each case. Caco-2 monolayers were treated with 2.5 mM EGTA, as described in Materials and Methods. Values are mean of 3 (PEG) or 7 (atenolol / PheAsp) experiments in each epithelia.

2 model epithelium was significantly different from rat intestine, both in terms of absolute permeability and the relationship with molecular size.

Literature data on the relative permeability of the paracellular route in small and large bowel is conflicting. The large bowel has generally been considered to be a "tighter" epithelium with higher electrical resistance and lower paracellular permeability (6) and, as a result, has been thought to contribute relatively little to passive drug absorption (15). However, Hollander and co-workers using *in vivo* perfusion studies in the rat have suggested that passive absorption of both large and small molecules is greater in the colon than the small bowel (7,8,16). The *in vitro* data presented here argues that for relatively small hydrophilic molecules the paracellular pathway in the colon has permeability characteristics similar to the ileum. This is supported by the electrical resistance data which after relating to the mucosal rather than the serosal surface area is comparable in both regions (Ileum—180 $\Omega.cm^2$; Colon—140 $\Omega.cm^2$). It has been suggested that the increased permeability to inulin in the colon may be due to the absorptive surface containing a higher proportion of "leaky" crypts than the ileum (7). This assumes that the lp of crypts in the colon is similar to that of the ileum. This is not supported by the present findings which show that while the small intestinal crypts have a high lp (91 m/cm^2) similar to that reported by other workers (4,9) the lp of colonic crypts is markedly lower (37 m/cm^2) and much closer to the value for villus enterocytes. Indeed, based on the relative lp's of crypt and villus/surface cells in each region and their relative contribution to total absorptive area available for paracellular transport there is no evidence that junctional density is an important variable in rat ileum and colon. In contrast, differences in the mucosal to serosal amplification ratio, actually determines the amount of junction available in each region and thus appears to be a much more important determinant of the extent of paracellular absorption.

When using morphometric parameters as correlates of permeability it will be important to consider how much of the mucosal surface area will be accessible to a drug in a complex structure such as the small intestine. For well absorbed compounds, it is likely that most of the absorption occurs in the upper part of the villus and these compounds will not diffuse very far into the intervillous space (17). However, solutes with low permeabilities, such as those used in the present study, are likely to diffuse throughout the intervillous space and so have access to the majority of the absorptive surface (18,19). Since many common hydrophilic drugs fall into this category, consideration of the effects of morphometric differences on the extent of absorption is clearly important, particularly when comparing different systems.

The morphometric data used here to "normalize" permeability in rat tissues would not take account of any regional differences in the pore size or "tightness" of the paracellular junctions such as that postulated by Fine *et al.* (20). However, significant differences in overall pore size between ileum and colon do not appear likely given the virtually identical relationship between permeability and molecular weight determined using PEG oligomers in the range 282 to 634. It has been postulated that there are different populations of paracellular pore sizes unevenly distributed along the length of the crypt/villus axis within the same region of the small intestine (21). This has not been addressed in the current study but could have an impact on the junctional area available for absorption of different sized molecules. Similarly, if the larger paracellular pores are located towards the base of the villous or in the crypts then larger molecules would have to diffuse further down the intervillous space in order to cross the epithelia resulting in a greater barrier to the permeability of these compounds.

To allow a more direct and absolute comparison of the paracellular pathways in rat small and large bowel, an *in vitro* system was chosen which would exclude many of the physical factors, particularly hydrodynamic factors, that appear to play a significant role in determining the extent of absorption *in vivo*. For example, increased fluid absorption and possible solvent drag in the colon compared to small bowel could explain the greater colonic absorption of inulin observed by *in vivo* perfusion (7). Similarly, differential effects of flow rate on the small and large bowel which may influence absorption by exposing different areas of the epithelium (20) are excluded. However, it is interesting to note that despite exclusion of these factors PEG permeability determined for ileum in this study correlates well with values (22) obtained by *in situ* ileal perfusion (Ileum *in vitro:* 8.4×10^{-6} cm/sec vs Ileum *in situ* perfusion: 11.7×10^{-6} cm/sec for PEG MW 502, values not adjusted for morphometric parameters).

The rationale for the use of Caco-2 as a model for predicting paracellular drug absorption is that it closely mimics the permeability profile of intestinal tissues (11). The evidence from this study is that while the rank order of permeability is similar in all three systems, there appear to be significant differences in the permeability characteristics of Caco-2 junctions compared to rat tissues. Even after normalization of values to take account of differences in the amount of paracellular pathway available and assuming that it is all accessible, the permeability of all three hydrophilic compounds was markedly lower across Caco-2 than rat ileum or colon. Furthermore, the discrepancy between Caco-2 and rat tissue increases markedly (from 4 to 40 fold) with increasing molecular weight over the range 282–634. Similar data has been presented by Artursson *et al.* (1993) (23). This is consistent with Caco-2 having smaller paracellular pores than rat intestine and is supported by the "normalized" R_t value for Caco-2 being 1.5-2 fold higher than intestinal tissue. These findings suggest that the accuracy with which Caco-2 can predict oral drug absorption may be critically dependent on the molecular size of the compounds being studied. Interestingly, when Caco-2 monolayers are treated with EGTA, a maneuver that increases paracellular permeability by opening tight junctions (13,24), both the absolute permeability and the size dependence are much closer to that of the intestinal tissues. Alternative cell lines with higher inherent junctional permeability than Caco-2 may offer distinct advantages for modeling and predicting paracellular drug absorption (13,25,26). It has also been reported that monolayers derived from low passage Caco-2 cells exhibit a lower electrical resistance accompanied by increased paracellular permeability (27) and an interesting question is whether these cells show a molecular weight discrimination closer to that of intestinal tissues.

It is possible that the permeability characteristics of rat intestine are different to human intestine and that this explains some of the discrepancy between rat and the human-derived Caco-2. A possible contributory factor may be the reported differences in size and shape of crypts and villi between species (28). Relatively few studies have directly compared permeabil-

ity in rat and human but the information available from studies in isolated intestinal sheets *in vitro* (27,29) and *in vivo* perfusion (30) suggests that the two species have broadly similar permeability characteristics.

In conclusion, when considering poorly absorbed compounds, normalizing permeability to take account of morphological variation in total absorptive surface and density of junctional pathways allows a more direct comparison of the permeability characteristics of different epithelial systems.

REFERENCES

1. I Bjarnason, A. Macpherson and D. Hollander. *Gastroenterology* **108**:1566–1581 (1995).
2. A Adson, P. S. Burton, T. J. Raub, C. L. Barsuhn, K. L. Audus and N. F. H. Ho. *J. Pharm. Sci.* **84**:1197–1204 (1995).
3. J. L Pappenheimer. *Am. J. Physiol.* **259**:G290–G299 (1990).
4. P. Claude. *J. Membrane Biol.* **39**:219–232 (1978).
5. Y. Tanaka, Y. Taki, T. Sakane, T. Nadai, H. Sezaki and S. Yamashita. *Pharm. Res.* **12**:523–528 (1995).
6. J. Spitz, G. Hecht, M. Taveras, E. Aoys and J. Alverdy. *Gastroenterology* **106**:35–41. (1994).
7. T. Y. Ma, D. Hollander, R. A. Erickson, H. Truong, H. Nguyen and P. Krugliak. *Gastroenterology* **108**:12–20 (1995).
8. P. Krugliak, D. Hollander, T. Y. Ma, D. Tran, V. D. Dadufalza, K. D. Katz and K. Lee. *Gastroenterology* **97**:1164–1170 (1989).
9. M. A. Marcial, S. L. Carlson and J. L. Madara. *J. Membrane Biology.* **80**:59–70 (1984).
10. C. S. Hyun, C. W. P. Chen, N. L. Shinowara, T. Palaia, F. S. Fallick, L. A. Martello, M. Mueenuddin, V. M. Donovan and S. Teichberg. *Gastroenterology* **109**:13–12 (1995).
11. P. Artursson *Crit. Revs. in Ther. Drug Systems* **8**:305–330 (1991).
12. G. Wilson, J. F. Hassam, C. J. Dix, I. Williamson, R. Shah, M. Mackay, and P. Artursson. *J. Control. Release* **11**:25–40 (1990).
13. A. Collett, E. Sims, D. Walker, Y-L. He, J. Ayrton, M. Rowland, and G. Warhurst. *Pharmaceutical Research* **13**:31–36 (1996).
14. S. B. Ruddy and B. W. Hadzija. *Drug Design. Disc.* **8**:207–210 (1991).
15. H. Lennernäs. *Pharm. Res.* **12**:1573–1582 (1995).
16. P. Krugliak, D. Hollander, C. C. Schlaepfer, H. Nguyen and T. Y. Ma. *Dig Dis and Sci* **39**:796–801 (1994).
17. R. P. Ferraris. In L. R. Johnson (ed.), *Physiology of the Gastrointestinal tract.* 3rd edition, Raven Press, New York, 1994, pp. 1821–1844.
18. M. D. Levitt, C. Fine, J. K. Furne and D. G. Levitt. *J. Clin Invest.* **97**:2308–2315 (1996).
19. R. E. Oliver, A. F. Jones and M. Rowland. Submitted for publication.
20. K. D. Fine, C. A. Santa, J. L. Porter and J. S. Fordtran. *Gastroenterology* **108**:983–989 (1995).
21. I. Bjarnsaon, A. MacPherson and D. Hollander, *Gastroenterology* **27**:721–726 (1992).
22. M. Kim. *J. Nutr.* **126**:2172–2178 (1996).
23. P. Artursson, A-L. Ungell and J-E Löfroth. *Pharm. Res.* **10**:1123–1129 (1993).
24. B. Gumbiner. *Am. J. Physiol.* **253**:C749–C758 (1987).
25. T. Y. Ma, D. Hollander, D. Bhalla, H. Nguyen and P. Krugliak. *J. Lab. Clin. Med.* **120**:329–341 (1992).
26. A. Adson, T. J. Raub, P. S. Burton, C. L. Barsuhn, A. R. Hilgers, K. L Audus and N. F. H. Ho. *J. Pharm. Sci.* **83**:1529–1536 (1994).
27. W. Rubas, M. E. M. Cromwell, Z. Shahrokh, J. Villagran, T-N. Nguyen, M. Wellton, T-H. Nguyen and R. J. Mrsny. *J. Pharm. Sci.* **85**:165–169 (1996).
28. J. L. Madara and J. S. Trier. In L. R. Johnson (ed.), *Physiology of the Gastrointestinal Tract.* 3rd edition, Raven Press, New York, 1994, pp 1577–1622.
29. P. B. Bijlsma, R. A. Peeters, J. A. Groot, P. R. Dekker, J. A. J. M. Taminiau and R. van der Meer. *Gastroenterology.* **108**:687–696, (1995).
30. F. A. Sutcliffe, S. A. Riley, B Kaser-Liard, L. A. Turnberg and M. Rowland. *Br. J. Pharmacol.* **26**:209P-207P (1988).